indole, 3-methylindole, 2,3-dimethylindole, and 1,2,3,4-tetrahydrocarbazole are 17.5, 13.5, 6.0, and 3.9 ns, respectively.[52] The latter compound is a W(1) analogue, which lacks the amino acid functional groups. The intersystem crossing rate in isolated indoles is relatively insensitive to methyl substitution, being 1.7×10^7, 2.5×10^7, and 2.8×10^7 s^{-1} for indole, 3-methylindole, and 2,3-dimethylindole.[50] The substantial drop of the fluorescence lifetime in the 2,3-dialkylindoles has been attributed to N-H bond rupture caused by coupling of the bound ^1L_b state with a dissociative ^1L_a state.[52] The N-H dissociation pathway may also make a small contribution to the nonradiative decay of indole in nonpolar solvents,[53] but there is no evidence for it in polar solvents.[12]

Less is known about the solution photophysics of methyl-substituted indoles. The lowest excited electronic state of most indole derivatives is ^1L_b in nonpolar and rigid polar solvents, but ^1L_a in polar fluid media.[4] However, in 2,3-dimethylindole ^1L_a is the lowest excited state even in nonpolar solvents.[54] In aqueous solution at 20 °C, indole, 3-methylindole, and 2,3-dimethylindole have monoexponential decays with lifetimes of 4.8, 9.4, and 4.3 ns.[6,14,15,55] The lifetime of 3-methylindole is independent of pH over the range pH 3-11.[17] The radiative rates calculated from quantum yield and lifetime data are $(4.8-5.2) \times 10^7$ s^{-1} for indole,[14,15], $(3.1-5.0) \times 10^7$ s^{-1} for 3-methylindole,[6,15,17,56] and 3.5×10^7 s^{-1} for 2,3-dimethylindole.[13,55] The estimated intersystem crossing rate is equal to the radiative rate in aqueous indole[12] and $\sim 3.3 \times 10^7$ s^{-1} in 3-methylindole.[17] W(1) is a 2,3-dialkylindole. Although the zwitterion has a somewhat longer lifetime than aqueous 2,3-dimethylindole, the 4.9-ns lifetime of the anion approaches the lifetime of 2,3-dimethylindole. This is opposite to the trend in tryptophan, where the zwitterion lifetimes are much shorter than the lifetime of 3-methylindole and the anion lifetime is about the same as 3-methylindole.[17] The complex fluorescence decays observed in many 3-substituted indoles are due to the functional groups on the alkyl side chain,[15,28,57] not the alkane moiety.

Acknowledgment. This work was supported by NIH grant GM35009.

Registry No. W, 73-22-3; W(1), 42438-90-4.

(53) Pernot, C.; Lindqvist, L. *J. Photochem.* **1976/1977**, *6*, 215-220.
(54) Strickland, E. H.; Billups, C.; Kay, E. *Biochemistry* **1972**, *11*, 3657-3662.
(55) Keating-Nakamoto, S. M.; Cherek, H.; Lakowicz, J. R. *Biophys. Chem.* **1986**, *24*, 79-95.
(56) Meech, S. R.; Phillips, D.; Lee, A. G. *Chem. Phys.* **1983**, *80*, 317-328.
(57) James, D. R.; Ware, W. R. *J. Phys. Chem.* **1985**, *89*, 5450-5458.

Conformational Studies of a Constrained Tryptophan Derivative: Implications for the Fluorescence Quenching Mechanism

William J. Colucci,[†] Luanne Tilstra,[‡] Melissa C. Sattler,[§] Frank R. Fronczek, and Mary D. Barkley*

Contribution from the Department of Chemistry, Louisiana State University, Baton Rouge, Louisiana 70803-1804. *Received May 18, 1990. Revised Manuscript Received August 10, 1990*

Abstract: The ground-state conformation of a rotationally constrained tryptophan derivative, 3-carboxy-1,2,3,4-tetrahydro-2-carboline, W(1), is determined from single-crystal X-ray diffraction, MM2 calculations, and ^1H NMR coupling constants. The solid-state structure represents the predominant solution conformation. W(1) populates only two minimum-energy conformations in solution, which correspond to the half-chair forms of cyclohexene. The conformers are distinguished mainly by distance of the carboxylate from the indole ring. The MM2-computed barrier for ring inversion in W(1) is 5.91 kcal/mol. The constrained tryptophan derivative and its ethyl ester, W(1)E, are used to investigate nonradiative decay pathways in tryptophan photophysics. The conformational restriction eliminates the excited-state intramolecular proton-transfer reaction observed with tryptophan (Saito, I.; Sugiyama, H.; Yamamoto, A.; Muramatsu, S.; Matsuura, T. *J. Am. Chem. Soc.* **1984**, *106*, 4286-4287). Global analysis of time-resolved fluorescence data reveals biexponential decays with lifetimes of 3.6 and 6.3 ns for the W(1) zwitterion and 2.9 and 4.8 ns for the W(1) anion. The relative amplitudes ($\alpha_1 = 0.12-0.20$ and $\alpha_2 = 0.88-0.80$) match the relative populations of the two conformers (0.3 and 0.7). Consequently, one lifetime is assigned to each conformer. The shorter lifetime component is associated with the conformer having the carboxylate closest to the indole ring. Esterification replaces the carboxylate of W(1) with a better electron acceptor and shortens both lifetimes, suggesting that intramolecular electron transfer may be an important mode of quenching. Arrhenius parameters concur that the temperature-dependent nonradiative process occurring in W(1) and W(1)E probably involves electron transfer.

Although the fluorescence of tryptophan is widely studied, its photophysics is not fully understood.[1,2] Numerous explanations have been proposed for the complex fluorescence decays of the tryptophan zwitterion as well as individual tryptophans in peptides and proteins. Several models for the biexponential decay of the tryptophan zwitterion are described in the preceding paper.[3] Among these the conformer model, which presumes emission from distinct, noninterconverting rotamers, is most frequently discussed.[4-7] Two nonradiative decay processes, intramolecular

[†] Present address: Ethyl Corp., Ethyl Technical Center, 8000 GSRI Ave., Baton Rouge, La 70820.
[‡] Present address: NIST, Bldg. 224, Rm. B-320, Gaithersburg, MD 20899.
[§] Present address: Dow Chemical USA, R&D Bldg. 2503, Box 400, Plaquemine, LA 70765-0400.

(1) Creed, D. *Photochem. Photobiol.* **1984**, *39*, 537-562.
(2) Beechem, J. M.; Brand, L. *Annu. Rev. Biochem.* **1985**, *54*, 43-71.
(3) Tilstra, L.; Sattler, M. C.; Cherry, W. R.; Barkley, M. D. *J. Am. Chem. Soc.*, preceding paper in this issue.
(4) Szabo, A. G.; Rayner, D. M. *J. Am. Chem. Soc.* **1980**, *102*, 554-563.
(5) Chang, M. C.; Petrich, J. W.; McDonald, D. B.; Fleming, G. R. *J. Am. Chem. Soc.* **1983**, *105*, 3819-3824.
(6) Petrich, J. W.; Chang, M. C.; McDonald, D. B.; Fleming, G. R. *J. Am. Chem. Soc.* **1983**, *105*, 3824-3832.

0002-7863/90/1512-9182$02.50/0

proton and electron transfer, are thought to account for the different lifetimes of various rotamers.[4,6,7-10] To test the conformer model, we synthesized a tryptophan derivative W(1) with restricted

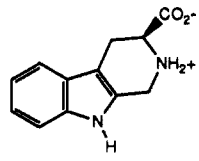

W(1)

rotation about the C^{α}–C^{β} and C^{β}–C^{γ} bonds and the amino group. The preceding paper suggested that the fluorescence decay of the W(1) zwitterion is biexponential.[3] The solution conformation of the constrained tryptophan must be known in order to define a one-to-one relationship between fluorescence lifetime and ground-state structure.

Single-crystal X-ray diffraction has been used to determine the conformation of a number of tryptophan derivatives.[11] Three rotamers about the C^{α}–C^{β} bond (χ_1 torsion) are observed. The most common is the $g(-)$ rotamer with the carboxylate anti to the indole ring. A few are $g(+)$ with the α-hydrogen anti to the ring. DL-tryptophan itself appears anomalous in adopting the t conformation with the ammonium in this position. The conformation about the C^{β}–C^{γ} bond (χ_2 torsion) shows more variability. However, the χ_2 torsion angle most often lies in the range of +80–115° (perpendicular conformation). Intermolecular hydrogen bonding in the crystal seems to be the most important determinant of side-chain conformation, although weaker intermolecular and intramolecular interactions may play a role. The solid-state structures represent some of the conformations available to the molecules in solution.

Molecular mechanics calculations have become an increasingly reliable method for solution structural analysis of small molecules.[12] For molecules such as amino acids, which may exhibit a high degree of charge localization, the ordinary bond dipole moments used to calculate dipole–dipole interaction energies may be unavailable or difficult to determine. This contribution to the overall force field can be replaced by an electrostatic potential, which then requires an estimate of all atomic point charges in the molecule. These charges have been estimated by using quantum mechanical approaches.[13-18]

NMR is unquestionably the most powerful experimental method for determining the structure of molecules in solution. The application of ^{1}H NMR to conformational analysis was pioneered by Karplus.[19] The well-known Karplus equation invokes a cosine-squared relationship between dihedral bond angles and coupling constants in ethane. For flexible molecules exhibiting multiple conformations, the experimentally observed vicinal coupling constant is actually a time-weighted average of individual coupling constants. At least in theory, individual coupling constants can be calculated for each available conformer.[20-23]

Previous studies have used ^{1}H NMR to determine rotamer populations of tryptophan[24,25] and tyrosine.[26] Tryptophan exhibits substantial rotational freedom about its C^{α}–C^{β} bond. Although the populations derived from different NMR methods (^3J couplings, NOE, and lanthanide perturbation) vary somewhat, all suggest predominance of the $g(-)$ rotamer (χ_1 torsion). In tryptophan the population of $g(-)$ ranges from 53 to 75% with the remaining rotamer populations distributed between $g(+)$ and t. The C^{β}–C^{γ} torsion (χ_2) occurs 80% in the perpendicular conformation.[25]

Previously we modified the Karplus equation to account for the total effect of molecular environment including solvent.[27] The angular dependence of the coupling constant is treated as a perturbation of the ethane system. Recently, Grassi and Pappalardo employed our modified version of the Karplus equation to assign unambiguously the ring conformations of three opioid analgesics.[28] Several groups subsequently showed that the combination of X-ray crystallography, ^{1}H NMR, and force field calculations complement each other in providing a more complete description of solution conformations in peracetylated glycals,[29] carnitine and acetylcarnitine,[21] a cyclic hexapeptide somatostatin analogue,[30] and the cyclodepsipeptide jasplakinolide.[23]

In this paper we determine the ground-state structure of the constrained tryptophan derivative W(1) from single-crystal X-ray diffraction, MM2 calculations, and ^{1}H NMR. We also use the constrained tryptophan to examine the role of nonradiative decay routes in the fluorescence decay. In particular, we confirm that the conformational restriction in W(1) precludes the best documented excited-state proton-transfer reaction.[9,10] We look for evidence of electron transfer from the excited indole ring to an electrophilic acceptor by substituting the carboxylate of W(1) with an ester group, which is a better electron acceptor. Finally, we discuss fluorescence quenching mechanisms in the constrained derivatives.

Experimental Section

Synthesis. The synthesis of 3-carboxy-1,2,3,4-tetrahydro-2-carboline, W(1), employed a modified Pictet–Spengler reaction described in the preceding paper.[3]

3-(Ethoxycarbonyl)-1,2,3,4-tetrahydro-2-carboline, W(1)E, from W(1). A 1.22-g (5 mmol) sample of W(1) was dissolved in 31 mL of

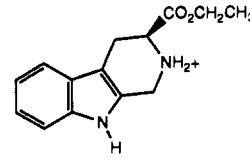

W(1)E

0.5 M ethanolic HCl and refluxed for 4 h. The volume was reduced to 15 mL by distillation, and 35 mL of absolute ethanol was added. After refluxing for another 4 h, the volume was reduced to 25 mL. The product crystallized as white needles at 5 °C (quantitative conversion except for a slight impurity that could not be completely removed by recrystallization). An 80-mg sample dissolved in 10 mL of ethanol was passed through a silica gel column (Baker, 60–200 mesh; 2.4 × 35 cm) eluted

(7) Engh, R. A.; Chen, L. X.-Q.; Fleming, G. R. *Chem. Phys. Lett.* **1986**, *126*, 365–372.
(8) Robbins, R. J.; Fleming, G. R.; Beddard, G. S.; Robinson, G. W.; Thistlethwaite, P. J.; Woolfe, G. J. *J. Am. Chem. Soc.* **1980**, *102*, 6271–6279.
(9) Saito, I.; Sugiyama, H.; Yamamoto, A.; Muramatsu, S.; Matsuura, T. *J. Am. Chem. Soc.* **1984**, *106*, 4286–4287.
(10) Shizuka, H.; Serizawa, M.; Shimo, T.; Saito, I.; Matsuura, T. *J. Am. Chem. Soc.* **1988**, *110*, 1930–1934.
(11) Bakke, O.; Mostad, A. *Acta Chem. Scand. B* **1980**, *34*, 559–570.
(12) Burkert, U.; Allinger, N. L. *Molecular Mechanics*; ACS Monograph Series 177; American Chemical Society: Washington, DC, 1982.
(13) Jug, K. *Theor. Chim. Acta* **1973**, *31*, 63–73.
(14) Flisza'r, S.; Goursot, A.; Dugas, H. *J. Am. Chem. Soc.* **1974**, *96*, 4358–4363.
(15) Julg, A. *Top. Curr. Chem.* **1975**, *58*, 1–37.
(16) Cox, S. R.; Williams, D. E. *J. Comput. Chem.* **1981**, *2*, 304–323.
(17) Abraham, R. J.; Hudson, B. *J. Comput. Chem.* **1985**, *6*, 173–181.
(18) Davis, M. E.; McCammon, J. A. *Chem. Rev.* **1990**, *90*, 509–521.
(19) Karplus, M. *J. Am. Chem. Soc.* **1963**, *85*, 2870–2871.
(20) Jamie, C.; Osawa, E.; Takeuchi, Y.; Camps, P. *J. Org. Chem.* **1983**, *48*, 4514–4519.
(21) Colucci, W. J.; Gandour, R. D.; Mooberry, E. A. *J. Am. Chem. Soc.* **1986**, *108*, 7141–7147.
(22) Ronchetti, F.; Toma, L. *Tetrahedron* **1986**, *42*, 6535–6540.
(23) Inman, W.; Crews, P. *J. Am. Chem. Soc.* **1989**, *111*, 2822–2829.
(24) Baici, A.; Rizzo, V.; Skrabal, P.; Luisi, P. L. *J. Am. Chem. Soc.* **1979**, *101*, 5171–5178.
(25) Dezube, B.; Dobson, C. M.; Teague, C. E. *J. Chem. Soc., Perkin Trans. 2* **1981**, 730–735.
(26) Laws, W. R.; Ross, J. B. A.; Wyssbrod, H. R.; Beechem, J. M.; Brand, L.; Sutherland, J. C. *Biochemistry* **1986**, *25*, 599–607.
(27) Colucci, W. J.; Jungk, S. J.; Gandour, R. D. *Magn. Reson. Chem.* **1985**, *23*, 335–343.
(28) Grassi, A.; Pappalardo, G. C.; Perly, B. *Magn. Reson. Chem.* **1988**, *26*, 693–700.
(29) Korytnyk, W.; Dodson-Simmons, O. *Molecular Basis of Cancer, Part B: Macromolecular Recognition, Chemotherapy, and Immunology*; Alan R. Liss: New York, 1985; pp 253–261.
(30) Kessler, H.; Bats, J. W.; Griesinger, C.; Koll, S.; Will, M.; Wagner, K. *J. Am. Chem. Soc.* **1988**, *110*, 1033–1049.

with ethanol. The product peak ran with the solvent front. Product was eluted as the free amine and was converted to the hydrochloride by adding a slight excess of ethanolic HCl to the combined fractions. The recovered dried solid yielded fluffy white needles when recrystallized from acetonitrile (50 mg, 62%): mp 269–270 °C (melting point of sublimed crystals with tube inserted at 250 °C); Anal. ($C_{14}H_{17}ClN_2O_2$) C, N, H calcd 6.10, found, 6.06; ^{1}H NMR (200 MHz, ref to DSS in D_2O, pD 3.6) δ 7.7–7.1 (d, d, m, Ar-H), 4.5 (dd, CH_2N, ^2J(HH) 16.2 Hz), 4.4 (q, CH_2O), 4.24 (dd, H_X), 3.40 (dd, H_A), 3.17 (dd, H_B), 1.37 (t, CH_3). TLC analysis [silica, ethanol/acetonitrile (1:1)] revealed a single spot when visualized by UV, iodine, and ninhydrin (R_f = 0.58). However, RP-HPLC (Bondapack C_{18}, 75% methanol/25% water) analysis showed two UV absorbing peaks; an unknown compound (2.9 min, 7.4% area) and W(1)E (7.9 min, 92% area). Alternative synthesis of W(1)E from tryptophan ethyl ester under Pictet-Spengler conditions and MS/MS were used to establish the source and identity of the impurity.

MS/MS. FAB mass spectrometry was performed as described in the preceding paper.[3] Mass spectrum of W(1)E·HCl synthesized from W(1) gave ions at m/z (relative intensity) 130 (10), 144 (90), 169 (20), 171 (15), 230 (17), 243 (7), 245 (100) $[M - Cl]^+$, 257 (10), 337 (7) $[M - Cl + Gly]^+$, and 489 (5) $[2M - 2Cl - H]^+$. Mass spectrum of W(1)-E·HCl synthesized from tryptophan ethyl ester gave ions at m/z (relative intensity) 74 (3), 102 (10), 130 (15), 144 (100), 169 (30), 171 (20), 230 (10), 243 (15), 245 (90) $[M - Cl]^+$, 257 (3), and 489 (10) $[2M - 2Cl - H]^+$. Collision-induced dissociation experiments showed that ions m/z 130, 169, 230, 243, and 257 do not derive from W(1)E, indicating impurities, with ions m/z 130 and 230 derived from ion m/z 257.

We believe that the impurities encountered in W(1)E·HCl result from autoxidation, which occurs upon exposure of the sample to air during handling. When a purified sample of W(1)E·HCl was left in the open air for several days, it turned yellow and showed multiple spots by TLC. Hence, the impurity in W(1)E·HCl with m/z 243 is interpreted as a two-electron oxidation product (−2H; dihydrocarboline), while the impurity with m/z 257 is produced from two further oxidations (−2H, +O; carboline *N*-oxide). No special precautions were taken in the RP-HPLC and MS/MS to protect the samples from air. A carefully purified sample, recrystallized three times from ethanol and stored under Ar at −20 °C in the dark, showed no evidence of impurities by TLC and NMR.

X-ray Diffraction. Single crystals of W(1) were grown from dilute aqueous $Ba(OH)_2$ solution by vapor diffusion with methanol at 4 °C. Intensity data were collected by ω–2θ scans of variable rate on an Enraf-Nonius CAD4 diffractometer equipped with Cu Kα radiation (λ = 1.541 84 Å) and a graphite monochromator. Crystal data: $C_{12}H_{12}N_2O_2 \cdot H_2O$, MW = 234.3, orthorhombic space group $P2_12_12_1$, a = 5.7232 (5) Å, b = 6.421 (2) Å, c = 30.666 (3) Å, V = 1126.9 (6) Å^3, Z = 4, D_c = 1.381 g cm^{-3}, μ(Cu Kα) = 7.9 cm^{-1}, T = 299 K, crystal size 0.06 × 0.32 × 0.44 mm. A full hemisphere of data within limits $4° < 2\theta < 150°$ was collected for $h < 4$, and one octant with $h > 3$. Scan rates varied 0.48–3.30° min^{-1}. Data reduction included corrections for background, Lorentz, polarization, and absorption. Absorption corrections were based on ψ scans, and the minimum relative transmission coefficient was 82.69%. Equivalent data were merged to yield 1984 unique data, of which 1807 had $I > 3\sigma(I)$ and were used in the refinement. The structure was solved by direct methods and refined by full-matrix least-squares analysis based on F with weights $w = \sigma^{-2}(F_o)$, using the Enraf-Nonius SDP programs. Non-hydrogen atoms were refined anisotropically, while hydrogen atoms were located from difference maps and refined isotropically. At convergence, R = 0.0414, R_w = 0.0469, GOF = 1.787 for 211 variables, and extinction = 4.5 (3) × 10^{-6}, and the maximum residual density was 0.37 e Å^{-3}. Refinement of the enantiomorphous structure yielded R = 0.0416, R_w = 0.0472, and GOF = 1.798. The difference in R_w is significant at α = 0.005, and the results of the former refinement are taken to represent the correct absolute configuration. Final coordinates are listed in Table I.

Molecular Mechanics. The molecular mechanics program MM2[31] was obtained from Quantum Chemical Program Exchange (Indiana University, No. 395) and was run on an IBM 3084QX6 computer. The program was modified to include a Morse potential instead of a cubic function to describe bond stretching energies.[21] The more realistic Morse potential prevents fictitious fragmentation of the molecule when driving through conformations with severe van der Waals interactions. In addition, the 1977 force field was updated with parameters from the 1985 version. Defined parameters, which involved mostly wild-card atoms, were taken primarily from corresponding atom types in the MM2 1985 force field. Because parameters for the N1-C2-C1-N2 [N(sp^2)-C(sp^2)-C(sp^3)-N(sp^3)] torsion were unavailable, they were set to zero. This is acceptable because the torsion is constrained within a ring. Default values were used for all parameters. Calculations were done at the dielectric constant of water at 25 °C, ϵ = 78.3.

(31) Allinger, N. L. *J. Am. Chem. Soc.* **1977**, *99*, 8127–8134.

Table I. Coordinates and Equivalent Isotropic Thermal Parameters

atom	x	y	z	B, Å^2
O1	0.7258 (3)	0.8910 (3)	0.72718 (4)	3.86 (3)
O2	0.7141 (3)	0.6834 (2)	0.66939 (4)	3.64 (2)
N1	1.4746 (3)	1.3696 (3)	0.61892 (4)	3.03 (3)
N2	1.0332 (3)	1.1503 (2)	0.69610 (4)	2.38 (2)
C1	1.1497 (3)	1.3321 (3)	0.67431 (5)	2.65 (3)
C2	1.3078 (3)	1.2506 (3)	0.63938 (5)	2.46 (3)
C3	1.2969 (3)	1.0563 (3)	0.62216 (4)	2.53 (3)
C4	1.1305 (3)	0.8930 (3)	0.63796 (5)	2.88 (3)
C5	0.9347 (3)	0.9958 (3)	0.66402 (5)	2.33 (3)
C6	0.7760 (3)	0.8437 (3)	0.68907 (5)	2.64 (3)
C7	1.4734 (3)	1.0481 (4)	0.58842 (5)	2.89 (3)
C8	1.5801 (3)	1.2458 (4)	0.58775 (5)	3.01 (3)
C9	1.7704 (4)	1.2903 (4)	0.56051 (5)	4.06 (4)
C10	1.8445 (4)	1.1323 (5)	0.53314 (6)	5.11 (5)
C11	1.7369 (4)	0.9378 (5)	0.53275 (6)	5.08 (5)
C12	1.5502 (4)	0.8911 (4)	0.56028 (5)	3.99 (4)
O1W	0.2893 (2)	0.9067 (2)	0.75910 (4)	3.10 (2)

Atomic point charges were calculated with the GAUSSIAN 82 series of programs[32] run on an FPS-264 advanced array processor interfaced to the IBM 3084QX6 mainframe computer. Charges were obtained directly from a Mulliken population analysis.[33] Initial MO coefficients for the zwitterion and anion forms of W(1) were determined at the STO-3G level.[34] Because computing the charges for all possible conformational states was impractical, calculations were performed only for coordinates determined from the crystal structure of the zwitterion. However, bond lengths involving hydrogen atoms were computed, because they appear shortened when hydrogen atoms are located by X-ray crystallography. Two anion forms were generated by removing one of the two hydrogen atoms attached to N2. MM2 calculations were performed on both anion forms and the zwitterion with atomic point charges that were determined from single-point calculations using the split valence 3-21G basis set.[35] The MO coefficients determined at the STO-3G level provided the initial guess for calculations employing the 3-21G basis set.

NMR. ^{1}H NMR spectra were recorded on a Bruker WP-200 FT-NMR at 300 K. For enhanced digital resolution the instrument was configured to give 0.153 Hz/point using a 32K block size. The W(1) solution was prepared by adding 5 mg to 0.5 mL of D_2O, pD 11.7. The W(1)E solution was prepared by dissolving 10 mg of the hydrochloride in 0.5 mL of D_2O, pD 3.6. Solution pDs were measured on a Radiometer Model PHM84 digital pH meter equipped with an Ingold Model 6030-30 NMR tube electrode and were calculated as meter reading +0.4 unit. Chemical shifts were measured relative to sodium 3-(trimethylsilyl)-1-propanesulfonate (DSS).

Chemical shifts and coupling constants were calculated by best fit to peak positions. Spectral simulations were performed on a Bruker ASPECT 3000 computer using the Bruker PANIC (1985) program, a minicomputer version of the LAOCOON-type program[36] used on large computers. Coupling constants for the dihedral angle ω were predicted as before[27]

$$^3J(\omega) = A + B\cos\omega + C\cos 2\omega + \cos\omega\,[(S_1 + S_4)\cos(\omega - 120) + (S_2 + S_3)\cos(\omega + 120)] \quad (1)$$

where the substituent constants S_i were determined from experimental coupling constants by

$$S_i = 4(A - {}^3J) \qquad i = 1, 2, 3, 4 \quad (2)$$

Substituents are defined in Figure 1. Literature values of the coupling constants of ethyl groups in the following monosubstituted ethanes were used in the study of W(1) and its ethyl ester: H, ethane, 8.0 Hz;[37] COO^-,

(32) Binkley, J. S.; Frisch, M. J.; deFres, D. J.; Raghavachan, K.; Whiteside, R. A.; Schelgel, H. B.; Fluder, E. M.; Pople, J. A. *Gaussian 82*; Carnegie Mellon Quantum Chemistry Publishing Unit: Pittsburgh, PA, 1983.
(33) Mulliken, R. S. *J. Chem. Phys.* **1955**, *23*, 1833–1840.
(34) Hehre, W. J.; Stewart, R. F.; Pople, J. A. *J. Chem. Phys.* **1969**, *51*, 2657–2664.
(35) Binkley, J. S.; Pople, J. A.; Hehre, W. J. *J. Am. Chem. Soc.* **1980**, *102*, 939–947.
(36) Costellano, S.; Bothner-By, A. A. *J. Chem. Phys.* **1964**, *41*, 3863–3869.
(37) Lynden-Bell, R. M.; Sheppard, N. *Proc. R. Soc. London A.* **1962**, *269*, 385–403.

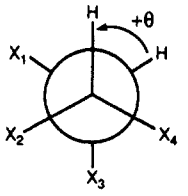

Figure 1. Newman projection showing the torsion angle convention and location of substituents used in eq 1.

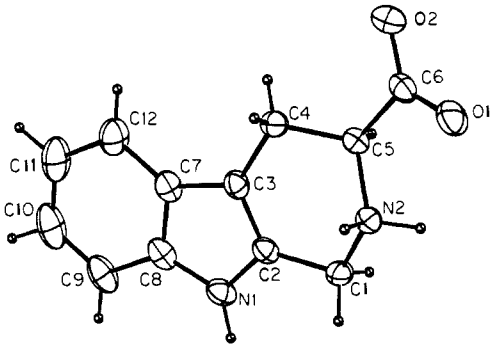

Figure 2. Molecular structure of W(1) zwitterion.

propionic acid in D_2O at pD 10.05, 7.66 Hz;[21] COOEt, ethyl propionate, 7.60 Hz;[27] N, triethylamine, 7.17 Hz;[27] N^+, trimethylethanaminium in D_2O at pD 2.41, 7.33 Hz;[21] C=C, 1-butene, 7.5 Hz.[27] The values of A, B, and C are not yet precisely known. Previously, the values determined from INDO calculations on ethane, $A = 8.37$, $B = -2.83$, and $C = 7.44$, were used.[21] However, these values do not adequately reproduce the observed coupling in ethane, which must yield A directly. Therefore, our approach in this work was to scale the INDO values to the experimentally observed coupling in ethane. Hence, values of $A = 8.00$, $B = -2.70$, and $C = 7.11$ were used in eqs 1 and 2.

Photochemical Isotope Exchange. H-D exchange was monitored on an IBM NR-100 FT-NMR spectrometer at ambient temperature. Solutions of tryptophan and W(1)E·HCl in unbuffered D_2O (5mg/0.5 mL) were irradiated with light from a 200-W Hg-Xe lamp filtered by a Corning UV transmitting/visible absorbing filter, No. 7-54. Under these conditions the half-life for exchange in tryptophan was ~30 min (literature value[9] of 5 min obtained with 400-W Hg lamp, Pyrex filter).

Steady-State and Time-Resolved Fluorescence. Fluorescence techniques are described in detail in the preceding paper.[3] The Photochemical Research Associates time-correlated single photon counting instrument was used with a picosecond dye laser excitation source.[38] Fluorescence decays were acquired in 512 channels of 0.0540 or 0.108 ns/channel to ~2.5 × 10^4 counts in the peak. W(1) and W(1)E·HCl were dissolved in 0.01 M phosphate buffer at the indicated pH. Solutions of W(1)E·HCl were made just before measurement to minimize autoxidation. Sample absorbance was <0.1 at 280 nm for steady-state measurements and <0.2 at 295 nm for time-resolved measurements.

Fluorescence decay data were analyzed as described in the preceding paper,[3] except that a term for scattered light was included to correct for Raman scattering from water at 330–340-nm emission wavelength.[39] The stability of the dye laser excitation source depended on ambient temperature as well as the chilled water temperature in the heat exchanger for the YAG laser power supply. Laser stability mostly affected the χ_r^2 values with little change in the values of the decay parameters. For the monoexponential *N*-acetyltryptophanamide standard χ_r^2 ranged from 1.0 to 1.25 on cooler days compared to 1.3–1.9 on warmer days. The high χ_r^2 values could not be lowered significantly by including more exponential terms in the fit. The decay parameters obtained from noisy data collected on warmer days were reproducible. Moreover, the same experiments repeated on cooler days gave almost identical values of the decay parameters.

Results and Discussion

X-ray Structure of W(1). It is clear from the equivalent C–O distances, C6–O1 1.241 (2) Å, C6–O2 1.244 (2) Å, the lack of electron density attributable to COOH hydrogen, and the protonation of N2 that W(1) crystallized in the zwitterion form. The configuration of the zwitterion and the atomic labeling are illustrated in Figure 2. This numbering scheme is used throughout the paper. The aromatic six-membered ring is planar to within 0.013 (2) Å, the five-membered ring is planar to within 0.007 (2) Å, and these planes form a dihedral angle of 2.80 (10)°. The heterocyclic six-membered ring has a half-chair conformation of local pseudosymmetry C_2, with a near-zero torsion angle about C2–C3 and local twofold axis bisecting C2–C3 and N2–C5. This ring is denoted the A ring in subsequent discussions. Carboxylate oxygen atom O2 is anti to the protonated nitrogen atom with a torsion angle N2–C5–C6–O2 of −167.19 (4)°. This conformation seems to be determined by intermolecular hydrogen bonding.

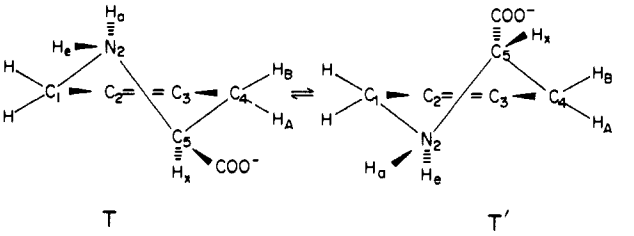

Figure 3. Representation of half-chair conformers of W(1) as viewed down the plane of the indole ring.

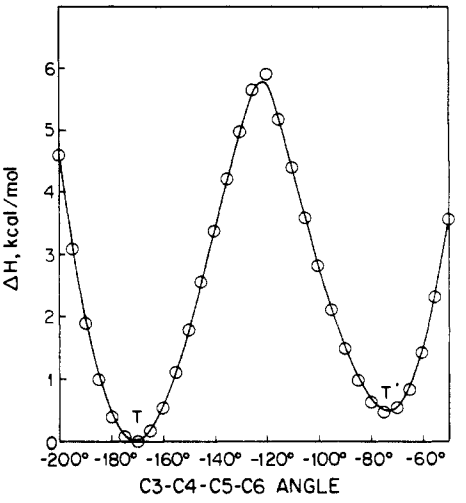

Figure 4. Torsional barrier for inversion of T and T′ conformers calculated by MM2.

The W(1) zwitterion is quite similar in structure to the racemic zwitterion 1,2,3,4-tetrahydroharmane-*cis*-3-carboxylic acid, 1-CH_3-W(1), which crystallized as the dihydrate.[40] The two molecules differ only by substitution of a methyl group at C1 and the bond distances agree well. The average difference in 18 bond distances is 0.006 Å, which is the magnitude of individual standard deviations in the 1-CH_3-W(1) structure. The largest difference, 0.021 (7) Å in C1–N2, is of borderline significance. The conformation of the A ring is almost congruent, with a mean endocyclic torsion angle difference between the two molecules of only 3.6° and a maximum individual difference of only 5.1°. However, the conformation of the carboxylate is slightly different. The N2–C5–C6–O2 torsion angle of 163.1° differs by 29.7° from the torsion angle in W(1), in order to maximize intermolecular hydrogen bonding with water molecules and other 1-CH_3-W(1) zwitterions.

Molecular Mechanics of W(1). The dihedral driver subroutine of the MM2 program was used to search for minimum enthalpy conformational states of W(1). The potential surface was explored by driving through various torsions formed by bonds in the A ring. Albeit only two minimum enthalpy structures could be found. Figure 3 illustrates the two conformers viewed down the plane of the indole ring. These structures correspond to the well-characterized half-chair forms of cyclohexene.[41] Higher enthalpy

(38) McMahon, L. P.; Colucci, W. J.; McLaughlin, M. L.; Barkley, M. D., in preparation.
(39) Kolber, Z. S.; Barkley, M. D. *Anal. Biochem.* **1986**, *152*, 6–21.
(40) Codding, P. W. *Can. J. Chem.* **1983**, *61*, 529–532.
(41) Anet, F. A. L.; Haq, M. Z. *J. Am. Chem. Soc.* **1965**, *87*, 3147–3150.

Table II. Comparison of Torsion Angles from the A Ring of W(1) Determined by X-ray and MM2

	zwitterion			anion			
torsion	X-ray	T	T′	T(H_e)[a]	T′(H_e)	T(H_a)[b]	T′(H_a)
C1-C2-C3-C4	−3.4	0.0	0.0	0.0	−0.2	0.1	0.1
C2-C3-C4-C5	17.9	19.7	−20.1	20.7	−20.8	20.0	−22.4
C3-C4-C5-N2	−46.7	−47.3	48.0	−48.1	48.8	−47.8	49.3
C4-C5-N2-C1	65.4	63.0	−64.0	62.8	−64.1	63.1	−64.1
C5-N2-C1-C2	−47.3	−43.5	44.1	−42.4	43.2	−43.0	42.9
N2-C1-C2-C3	17.3	10.6	−10.5	9.5	−9.7	10.1	−9.2
C3-C4-C5-C6	−169.5	−170.6	−75.0	−171.3	−74.1	−171.0	−73.6

[a] Anion formed by removal of H_a (Figure 3) bonded to N2. [b] Anion formed by removal of H_e (Figure 3) bonded to N2.

Table III. Enthalpies and Populations of W(1) Determined from Molecular Mechanics Calculations

ionizatn state	conformer	relative enthalpy[a]	populatns[b]	combined T and T′ populations
zwitterion	T	0.00	0.69	0.69
	T′	0.48	0.31	0.31
anion	T(H_a)	0.00	0.35	
	T(H_e)	0.01	0.34	0.69
	T′(H_a)	0.37	0.19	
	T′(H_e)	0.64	0.12	0.31

[a] Relative enthalpies (kcal/mol) were determined at the minimum of the potential well (Figure 4). [b] Populations were determined from a Boltzmann distribution calculated at 298 K.

boat forms could not be located by any of the driver calculations. It is possible that the energy surface near the boat form is very shallow, causing the molecule to slip easily into the half-chair forms. The minimization of the STO-3G structure yielded conformer T directly. Except for rotation of the carboxylate, which differs from the W(1) crystal structure by ~45°, this conformer corresponds to the crystal structure. The second structure, T′, could be located most directly by driving the C3-C4-C5-C6 torsion from −170° near the T conformation to −60° in 5° increments. The torsional barrier between the T and T′ conformations of the zwitterion was determined by driving in both directions. The barrier for ring inversion shown in Figure 4 is $\Delta H^{\ddagger}$ = 5.91 kcal/mol. This value is similar to $\Delta G^{\ddagger}$ values determined for 4-substituted cyclohexenes, which range from 5.3 to 6.5 kcal/mol.[42]

Statistical comparison of bond lengths, bond angles, and torsion angles in the T conformer and the X-ray structure shows good agreement between the two structures and lends credence to the MM2 force field. Table II gives the values of the torsion angles in the A ring for the zwitterion and anion forms of the T and T′ conformers of W(1). The torsion angles for the zwitterion determined from the X-ray structure are included for comparison. The similarity between the X-ray and MM2 structures for the T conformer is independent of ionization state. Likewise, the MM2 structures of the T′ conformer are all remarkably homologous.

The enthalpies and populations of the two conformers of W(1) are shown in Table III. The T conformer represents the global minimum corresponding to the crystal structure. The T′ conformer is always of higher enthalpy regardless of charge state. The calculated populations of T and T′ conformers in the zwitterion are 69 and 31%, respectively. In the anion, the populations of the T and T′ conformers are each partitioned between the H_a and H_e forms. However, the combined populations of the H_a and H_e forms of the anion give the same relative population of T and T′ conformers as the zwitterion. The preponderance of the T conformer probably arises from the greater stability of the pseudoequatorial carboxylate compared to the pseudoaxial carboxylate in the T′ conformer. While force field calculations may predict accurate geometric structures, the relative energy between structures will not necessarily be correct. Most important is the degree to which the force field is able to account for solvation.

Table IV. Conformers and Populations of W(1) and W(1)E Determined by ^{1}H NMR Coupling Constants

	W(1)	W(1)E	
	pD 11.7, D_2O	pD 3.6, D_2O	CD_2Cl_2[d]
J_{AX}, Hz	4.3	5.1	5.0
J_{BX}, Hz	10.6	10.6	9.7
ω_T,[a] deg	−48	−48	−48
$\omega_{T'}$,[b] deg	40	29	28
P_T,[c] %	73	70	65

[a] ω_T is the C3-C4-C5-N2 torsion angle of the T conformer determined by MM2 calculations on W(1). [b] $\omega_{T'}$ is the C3-C4-C5-N2 torsion angle of the T′ conformer calculated from coupling constants by using eqs 3. [c] Population of the T conformer calculated from coupling constants by using eqs 3. [d] Coupling constants for the free base form of W(1)E from ref 43.

In our work we rely upon the congruence between MM2 and NMR results as the ultimate test of the validity of the populations resulting from computed energies.

^{1}H NMR of W(1) and W(1)E. The ^{1}H NMR spectra of W(1) and W(1)E were recorded at 200 MHz [data for W(1) in ref 3]. The protons attached to C4 and C5 appeared as a series of three distinct quartets indicative of simple ABX systems. Absolute assignment of the diastereotopic H_A and H_B protons was based on vicinal coupling constants. The largest ^3J(HH) must be assigned to H_B, which is antiperiplanar to H_X in the T conformer. The coupling constants $^3J_{AX}$ and $^3J_{BX}$ given in Table IV were taken directly from spectral simulations as discussed in the Experimental Section. The root mean square errors for the fits involving ABX systems of W(1) and W(1)E were 0.131 and 0.114 Hz, respectively.

Conformers and populations of W(1) and W(1)E were calculated from the ^{1}H NMR data by simultaneous solution of eqs 3

$$^3J_{AX} = \sum_i P_i {}^3J_{AX}(\omega_i) \quad (3a)$$

$$^3J_{BX} = \sum_i P_i {}^3J_{BX}(\omega_i) \quad (3b)$$

$$\sum_i P_i = 1 \quad (3c)$$

as described previously for ABX systems.[21] With only two coupling constants, the solution is underdetermined. Fortunately, the molecular mechanics calculations strongly suggest that the total number of possible conformers is only two. Hence, the dihedral angle and population of one conformer may be determined if the angle of the other conformer is fixed at the value computed by MM2. The dihedral angles ω_i in eq 1, which represent the torsion angles between coupled hydrogens, were expressed in terms of the C3-C4-C5-N2 angles, ω_T and $\omega_{T'}$. Because the X-ray and MM2 structures gave good agreement for the value of ω_T in the zwitterion (Table II), we chose ω_T as the fixed angle. Its value was set to −48°, which is the computed value for the W(1) anion. This is the ionization state present in the ^{1}H NMR experiment.

Table IV shows the results obtained for W(1) in alkaline D_2O, and for W(1)E in acidic D_2O and in CD_2Cl_2.[43] The 40° dihedral angle obtained for the T′ conformer of W(1) compares favorably with the two values, 48.8° and 49.3°, computed for the H_e and H_a forms of the anion by MM2 (Table II). The experimental and calculated populations of W(1) conformers are also in good

(42) Jensen, F. R.; Bushweller, C. H. *J. Am. Chem. Soc.* **1969**, *91*, 5774-5782.

(43) Plate, R.; Nivard, R. J. F.; Ottenheijm, H. C. J. *Heterocycles* **1986**, *24*, 3105-3114.

Table V. Time-Resolved Emission Spectral Data for W(1) and W(1)E at 25 °C[a]

	α_1(350 nm)	τ_1, ns	τ_2, ns	χ_r^2	ν_{cg}^{-1}, nm 1	2
W(1)						
pH 5.5[b]		6.12		2.51		
	0.12	3.62	6.35	1.83	339	339
pH 10.5[c]		4.52		3.17		
	0.20	2.88	4.78	1.24	343	359
W(1)E						
pH 6.0[d]		4.13		18.7		
	0.46	2.37	5.00	1.31		
	0.36[e]	2.09	4.58	1.09	348	350

[a] 295-nm excitation wavelength. Global analysis of experiments at 5-nm intervals. [b] 315–375 nm. [c] 320–395 nm. [d] 330–375 nm. [e] Results from triple-exponential fit with relative amplitudes corrected for 1% of an 11.44-ns component.

agreement: 73% T conformer determined by NMR and 69% computed by MM2 (Table III). Hence the MM2 and ^{1}H NMR methods have converged upon the same result.

The coupling constants for W(1)E were also analyzed by setting ω_T to −48°. Although an exact value of ω_T for W(1)E was not computed, esterification is expected to have only a minor influence on the A ring in the T conformer. A dihedral angle of ~30° was obtained for the T′ conformer of the W(1)E cation (Table IV). The smaller value indicates a more flattened ring in the ethyl ester compared to W(1), which might result from increased steric repulsion for the pseudoaxial ethoxycarbonyl group in the T′ conformer. It is interesting to note that changing the solvent polarity from D_2O to CD_2CL_2 only shifts the population of conformers by 5% without affecting the conformation of the A ring.

Photochemical Isotope Exchange. Saito et al.[9] previously demonstrated a highly efficient and selective intramolecular proton-transfer reaction in tryptophan. When tryptophan zwitterion is excited by a mercury lamp, H–D exchange of the C4 aromatic proton is observed by ^{1}H NMR. The exchange is quenched by iodide ion consistent with proton transfer from the singlet excited state. In the proposed mechanism for the photosubstitution the ammonium loops back over the indole ring and initiates the exchange. The stereochemical constraint in W(1) precludes such conformations. If the Saito mechanism is correct, the intramolecular excited-state proton-transfer reaction seen in tryptophan should not occur in W(1).

The photochemical isotope-exchange experiment was done in the W(1)E cation, because the W(1) zwitterion is not sufficiently soluble for NMR experiments. No significant proton exchange was observed at pD 3.6 at the C12 position in the aromatic six-membered ring of W(1)E (equivalent to C4 in indole) during 3 h of irradiation. In contrast, H–D exchange at the C4 position of indole occurred in tryptophan with a half-life of 30 min under the same experimental conditions. The tryptophan ethyl ester cation did not show exchange at C4 because of its subnanosecond fluorescence lifetime. All three compounds gave low levels of the slow H–D exchange at other aromatic positions noted by Saito et al.[9] The fluorescence lifetimes of W(1) and W(1)E are longer than the lifetimes of tryptophan (Table V). Hence the absence of H–D exchange at C12 of W(1)E supports our prediction that excited-state intramolecular proton transfer does not take place in W(1).

Time-Resolved Fluorescence of W(1) and W(1)E. Fluorescence lifetime data for the W(1) zwitterion and anion at 25 °C are summarized in Table V. The results in the table were obtained from global analyses of time-resolved emission spectral data (Figure 5). In both cases biexponential fits gave lower χ_r^2 values and randomly fluctuating autocorrelation functions.[44] The

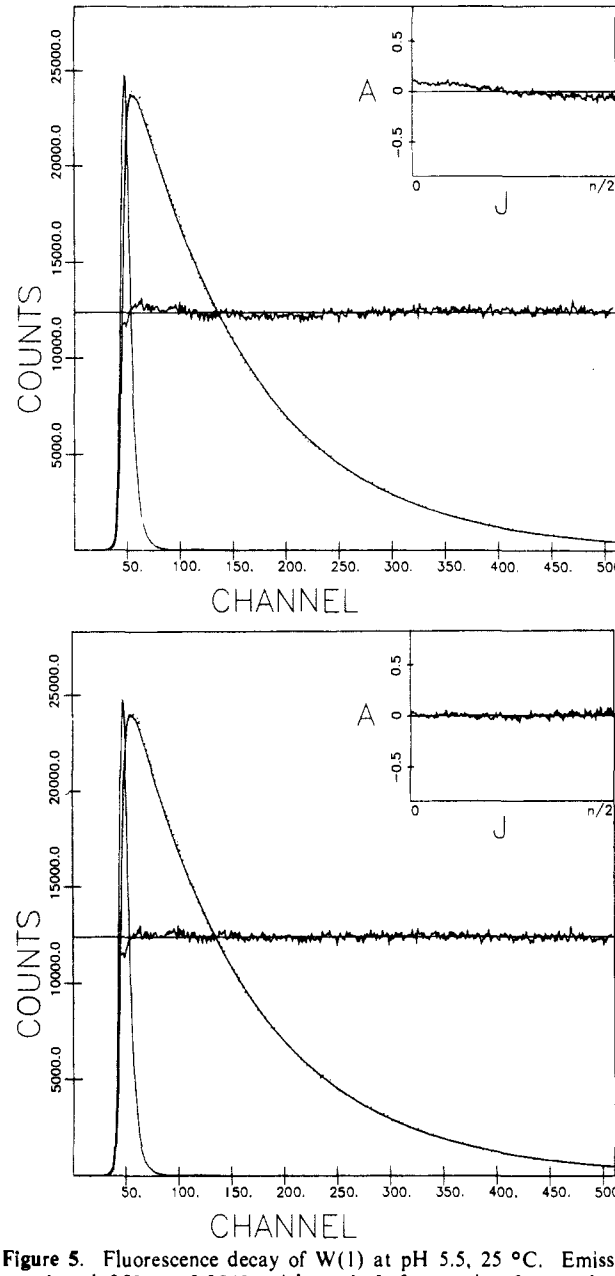

Figure 5. Fluorescence decay of W(1) at pH 5.5, 25 °C. Emission wavelength 350 nm, 0.0540 ns/channel. Left curve is reference decay. Dotted line is sample decay; smooth curve through points is best fit to the following: (upper) single-exponential function, τ = 6.12 ns; partial χ_r^2 = 1.87. (lower) double-exponential function, α_1 = 0.12, τ_1 = 3.62 ns, α_2 = 0.88, τ_2 = 6.35 ns; partial χ_r^2 = 1.60. Weighted percent residuals and autocorrelation function of the residuals (inset) are also shown.

lifetimes are 3.6 and 6.3 ns for the zwitterion[45] and 2.9 and 4.8 ns for the anion. The relative amplitudes of the two exponential decays are about the same in the W(1) zwitterion and anion. In the case of ground-state heterogeneity, the amplitudes are proportional to the molar extinction spectrum, fluorescence emission spectrum, radiative rate, and concentration of the different fluorescent species. The steady-state emission spectrum of W(1) is independent of excitation wavelength, indicating that the extinction coefficients and radiative rates of the two components are similar. The decay-associated emission spectra of the two

(44) The data in the preceding paper[3] were collected with a nanosecond flashlamp excitation source. The instrumental response was wider with a longer tail and the number of counts in the decay curves was lower in the flashlamp experiments. The cleaner pulse and better counting statistics in the laser experiments facilitate the resolution of the closely spaced biexponential decays.

(45) Dr. Maurice R. Eftink independently made time-resolved fluorescence measurements on W(1) at pH 5.1, 20 °C, using laser excitation at 295 nm. Both time-domain and frequency-domain experiments gave biexponential decays. Decay parameters were as follows: α_1 = 0.05, τ_1 = 2.05 ns, τ_2 = 6.35 ns from time-correlated single photon counting data; α_1(340 nm) = 0.36, τ_1 = 0.97 ns, τ_2 = 6.69 ns from global analysis of variable frequency phase data acquired at five emission wavelengths.

components are shifted little if at all relative to each other (Table V). We therefore assume that the amplitudes depend mainly on the mole fraction of the two species. Because the relative amplitudes $\alpha_1 = 0.12-0.20$ and $\alpha_2 = 0.88-0.80$ of the exponential decays match the relative populations 0.3 and 0.7 of the two conformers identified in the previous section, it is reasonable to assign one lifetime to each conformer. Accordingly, the major decay component with the longer lifetime would represent the T conformer with the pseudoequatorial carboxylate. The minor decay component with the shorter lifetime would correspond to the T′ conformer with the pseudoaxial carboxylate.

Intramolecular electron transfer from the excited indole donor to the carboxylate has been proposed to occur in tryptophan.[4,6] According to semiclassical theory,[46] the rate of electron transfer drops off exponentially with increasing distance between donor and acceptor. In W(1) the distance between the indole ring and the amino group is the same in both conformers. However, the carboxylate is closer to the indole ring in the T′ conformer than in the T conformer. Through-space electron transfer to the carbonyl should be faster in the T′ conformer, shortening its fluorescence lifetime. We argued above based on relative populations that the minor decay component with the shorter lifetime corresponds to the T′ conformer. The rate of electron transfer also depends on the driving force for the electron-transfer reaction. The ester substitution in W(1)E replaces the carboxylate with a more electrophilic group.[47] This should shorten the fluorescence lifetime of both conformers if electron transfer occurs in these compounds.

The absorption and emission spectra of W(1)E closely resemble the spectra of W(1) shown in the preceding paper.[3] In the absorption spectrum of both W(1) and W(1)E cations, the peak at 270 nm is a little higher than the peak at 276 nm (not shown). As before, the pK of the amino group in W(1)E was determined at 25 °C from the absorbance change at 278 nm. The pK of 7.9 is nearly 1 pH unit below the pK of W(1). The emission spectrum of the W(1)E free base (not shown) is blue-shifted 6 nm relative to the spectrum of the W(1) anion. The quantum yield of the W(1)E cation was 0.22 at pH 6.0, which is only 54% of the value for the W(1) zwitterion at pH 7.0.

Table V also gives fluorescence lifetime data for the W(1)E cation at 25 °C. The global χ_r^2 of 18 for a single-exponential fit was clearly unacceptable. A double-exponential function gave an adequate fit with a global χ_r^2 of 1.3. As anticipated, the 2.4- and 5.0-ns values for the lifetimes of W(1)E were shorter than the 3.6- and 6.3-ns lifetimes of the W(1) zwitterion. Three exponential decays could not be resolved in single-curve analyses but were resolved by global analysis with little change in χ_r^2 and randomness of the autocorrelation function. Including a third component of 11.4-ns lifetime and 1% amplitude dropped the lifetimes of the other two components to 2.1 and 4.6 ns, respectively, and improved the agreement between their amplitudes and the conformer populations. The third decay component may represent an artifact of the data analysis or possibly the impurity in W(1)E noted in the Experimental Section.

The fluorescence decay of the W(1)E cation was measured at 5 °C intervals over the temperature range 5–45 °C. Decay curves were collected at 350-nm emission wavelength and were fitted to double-exponential functions with χ_r^2 values of 0.92–1.18. The lifetimes decreased with increasing temperature, but the relative amplitudes fluctuated around $\alpha_1 = 0.3-0.4$ and $\alpha_2 = 0.7-0.6$, suggesting that they are independent of temperature. The data at each temperature were reanalyzed by assuming fixed amplitude ratios α_1/α_2 of 0.3/0.7 and 0.4/0.6. The amplitude ratio $\alpha_1/\alpha_2 = 0.4/0.6$ gave somewhat better fits with χ_r^2 values of 1.06–1.46. The temperature dependence of the lifetimes τ_i obtained from the latter fits was analyzed as described for W(1) in the preceding paper.[3] The lifetimes of W(1)E were fit to the Arrhenius equation $\tau_i^{-1} = k_{oi} + A_i \exp(-E_i^*/RT)$, where k_{oi} is the temperature-independent rate, A_i is the frequency factor, and E_i^* is the activation energy of component i. Plots of $\ln(\tau_i^{-1} - k_{oi})$ vs $(RT)^{-1}$ were constructed by using our previous estimate of $k_{oi} = 9.9 \times 10^7$ s^{-1} (Figure 6). The Arrhenius plot for the longer lifetime component τ_2 is linear and gives essentially the same values for A_2 and E_2^* as a fit to the nonlinear equation without assuming a value for k_{o2}. Less satisfactory results were obtained from both linear and nonlinear fitting procedures for the shorter lifetime component τ_1. Presumably this is due to greater scatter in the lifetime values of the minor decay component. The k_o, A, and E^* values for W(1)E are summarized in Table VI together with the results for W(1).

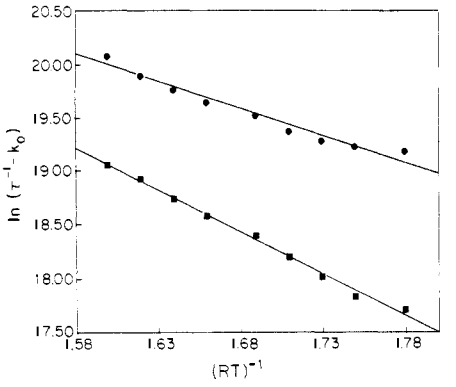

Figure 6. Linear least-squares fit of temperature dependence of fluorescence lifetimes of W(1)E at pH 6.0 to Arrhenius equation, $\ln(\tau^{-1} - k_o) = \ln A - E^*/RT$, assuming $k_o = 9.9 \times 10^7$ s^{-1}. (●) τ_1; (■) τ_2.

Table VI. Summary of Arrhenius Parameters

	k_o, s^{-1}	A, s^{-1}	E^*, kcal/mol
W(1)[a]			
linear fit	9.9×10^7	3.1×10^{11}	5.0
nonlinear fit	1.25×10^8	3.7×10^{13}	8.1
W(1)E,[b] τ_1			
linear fit	9.9×10^7	1.6×10^{12}	5.0
nonlinear fit	2.7×10^8	7.3×10^{16}	12.0
W(1)E,[b] τ_2			
linear fit	9.9×10^7	4.8×10^{13}	7.8
nonlinear fit	1.02×10^8	7.8×10^{13}	8.1

[a] Data from ref 3 at pH 7.0, 296-nm excitation wavelength, 345-nm emission wavelength. [b] pH 6.0, 295-nm excitation wavelength, 350-nm emission wavelength.

Conclusions

In this paper we used two rotationally constrained analogues of tryptophan, W(1) and its ethyl ester W(1)E, to investigate nonradiative pathways in the fluorescence decay of tryptophan. We first thoroughly characterized the ground-state conformation of W(1). Both molecular mechanics and ^{1}H NMR methods converged upon essentially the same result, suggesting that in solution the molecule populates only two conformations. These structures correspond to the half-chair forms of cyclohexene. They are related by twisting of the A ring and are distinguished by the distance of their carboxylates from the indole ring. The solid-state structure of W(1), which was determined by X-ray diffraction, represents the most stable conformation available to the molecule in solution. We then showed that the excited-state intramolecular proton-transfer reaction observed in tryptophan[9,10] does not occur in the constrained derivatives. The absence of photochemically induced H–D exchange at C12 of W(1)E (equivalent to C4 of indole) supports the mechanism proposed by Saito et al.,[9] in which the ammonium loops back over the indole ring and initiates the exchange. By the same argument, the stereochemical constraint excludes other proposed intramolecular quenching mechanisms such as ring protonation at the C2 position[48] or formation of a σ complex at C12.[47] Global analysis of time-resolved emission spectral data for both W(1) andW(1)E revealed biexponential

(46) Marcus, R. A.; Sutin, N. *Biochim. Biophys. Acta* **1985**, *811*, 265–322.
(47) Ricci, R. W.; Nesta, J. M. *J. Phys. Chem.* **1976**, *80*, 974–980.
(48) Ricci, R. W. *Photochem. Photobiol.* **1970**, *12*, 65–75.

decays. The ester group shortens the lifetimes. The drop in mean lifetime parallels the drop in quantum yield, indicating a change in nonradiative decay rate. Because the amplitudes of the two decay components correspond to the relative populations of the two conformers, we assigned one lifetime to each conformer.

Clearly, discrete fluorescence lifetimes may arise from unique conformers of W(1) only if the conformers do not interconvert during the lifetimes of their excited states. The rate of inversion of the cyclohexene half-chair is very fast in the ground state. Experimental values for 4-substituted derivatives in nonpolar solvents at 25 °C are in the range 1–10 ns.[41,42] While we did not explicitly compute the T and T′ inversion rates, we may estimate them from transition-state theory

$$k_{T\text{-}T'} = \kappa(kT/h)\exp(-\Delta G^{\ddagger}/RT) \qquad (4)$$

where k is the Boltzmann constant, T is absolute temperature, and h is Planck's constant. Symmetry arguments suggest that the entropy of activation for half-chair interconversion is zero,[41] so $\Delta G^{\ddagger}$ would equal the calculated barrier height of 5.91 kcal/mol for W(1). Unfortunately it is difficult to assign a value to the transmission coefficient, κ, which incorporates all correction factors and uncertainties. Using stochastic molecular dynamics simulation, Kuharski et al.[49] computed a value of 0.4 for cyclohexane isomerization in a low viscosity solvent. If we take $\kappa = 0.4$, then the average lifetimes of the T and T′ conformers before inversion would be 8.9 and 3.9 ns at 25 °C, respectively. However, unlike the hydrocarbon rings, W(1) can have sizable interactions with hydrogen-bonding solvents, which might reduce the transmission coefficient further. Also, the barrier may be higher in the excited state than in the ground state, because the C2–C3 bond in indole derivatives has less π electron density in the ^1L_a state.[50] For example, $\Delta G^{\ddagger} = 10.7$ kcal/mol for ring inversion in cyclohexane.[51] Increasing the barrier in W(1) by just 1 kcal/mol gives lifetimes of 48 and 21 ns. Hence, the estimated conformer lifetimes should probably be regarded as lower limits.

For tryptophan and related compounds, multiple quenching mechanisms contribute to the nonradiative rate. The observed Arrhenius parameters are conglomerates of frequency factors A and activation energies E^* for all of the temperature-dependent nonradiative processes. These include quenching intrinsic to the indole moiety plus any intramolecular quenching due to functional groups acting separately or in common. For example, Fleming and co-workers[6,8] deduced the intrinsic quenching in tryptophan from the nonradiative rate of 3-methylindole. In 3-methylindole, the large frequency factor ($A = 10^{17}$ s^{-1}) and activation energy ($E^* = 13$ kcal/mol) were attributed to photoionization.[8,52] Indeed, very large A values are suggestive of electronic rather than nuclear motion. However, monophotonic ionization of tryptophan occurs from S_1 with a quantum yield of 0.075 at pH 7,[53] which is insufficient to account for all of the temperature-dependent quenching. The Arrhenius parameters for tryptophan at pH 11 ($A = 6.1 \times 10^{16}$ s^{-1} and $E^* = 12.3$ kcal/mol)[5,8] are nearly identical with 3-methylindole, indicating that only intrinsic mechanisms are operating at high pH.

A second nonradiative process involving electron transfer from the excited indole ring has also been proposed to occur in tryptophan.[5,6,8,52] This temperature-dependent quenching mechanism is distinguished from photoionization in requiring electron capture by an electrophilic group. Carboxylate is considered to be a very poor electron acceptor, though its acceptor ability may be greatly enhanced by an adjacent ammonium.[4-6,47,54] The frequency factor and activation energy for this process are expected to be smaller than for photoionization.[55] Hence, for tryptophan at neutral pH, A drops to 3×10^{13} s^{-1} and E^* to 6.7 kcal/mol.[5,56] While this may result from increased electron transfer, it is also at least partly due to the intramolecular proton transfer that occurs in the zwitterion.[9] Shizuka et al.[57] showed through temperature studies of tryptamine in MeOH–H_2O (9:1) that A and E^* for the intramolecular proton transfer may be as low as 3.8×10^{11} s^{-1} and 4.1 kcal/mol, respectively. When the total nonradiative rate for tryptamine in water at pH 5 is considered, $A = 2.5 \times 10^{14}$ s^{-1} and $E^* = 8.9$ kcal/mol,[52] suggesting substantial but not solely intrinsic quenching of the indole.

The Arrhenius data for W(1) and its ester allow us to probe temperature-dependent processes in the absence of intramolecular proton transfer. Except for the nonlinear fit for τ_1 of W(1)E (Table VI), which is most likely an artifact caused by noisy data for the shorter lifetime component, the values of A and E^* for W(1) and W(1)E fall in the range observed for tryptophan at pH 6–7 (see above) and indole-3-acetic acid ethyl ester ($A = 4.4 \times 10^{13}$ s^{-1} and $E^* = 7.1$ kcal/mol).[52] We can conclude that the intrinsic process seen in 3-methylindole is a minor pathway for quenching of W(1) or W(1)E, as it is for tryptophan at pH 6–7. Also, note that the Arrhenius parameters for indole-3-acetate ($A = 1.3 \times 10^{17}$ s^{-1} and $E^* = 12.8$ kcal/mol) and its ethyl ester (see above) are distinctly different,[52] but those for W(1) and its ester are about equal. Apparently, the ammonium enables the carboxylate to play a quenching role, which at least resembles that of the ester. As stated above, intramolecular proton transfer or other conformationally dependent mechanisms cannot be invoked to explain these observations. Thus, the temperature-dependent process occurring in both W(1) and W(1)E must involve electron transfer. Otherwise, an as yet unidentified mechanism is extant.

Assuming that conformer interconversion is slow compared to the excited-state lifetime, we have demonstrated a one-to-one correspondence between ground-state conformers and fluorescence lifetimes of W(1) and its ethyl ester. Even if ring inversion does occur in the excited state, we can still conclude that the fluorescence lifetimes of the two conformers are different. However, the amplitudes and decay rates of the biexponential functions woud not be simply related to populations and lifetimes of conformers. Structurally, the two conformers are distinguished by the distance of the carboxylate from the indole ring. We now address the question of why the fluorescence lifetimes of W(1) and W(1)E are shorter in the T′ conformer than in the T conformer. We make the usual assumption that the radiative rate k_r is about the same in both conformers, so the different lifetimes are due mostly to nonradiative processes. This is justified because a wide variety of indole derivatives have remarkably similar radiative rates in the range $k_r = (4\text{–}7) \times 10^7$ s^{-1}.[3,4,6,52] We therefore consider various nonradiative decay routes. Excited-state deprotonation of the indole NH is only possible at high pH.[58] Moreover, it is unlikely that this mode of quenching would be sensitive to conformation of the A ring. Excited-state intramolecular proton transfer and photoionization have been eliminated as possible mechanisms, although these processes are likely in tryptophan and simpler indoles. Other possible ring protonation reactions are excluded by the absence of a solvent isotope effect.[59] Förster and Dexter energy-transfer mechanisms can be ruled out because of negligible spectral overlap between the emission of W(1) and W(1)E and the absorption of carboxylate and ethyl ester, respectively.[60] Of course, internal conversion and intersystem crossing are occurring, but the effects of conformation and ground-state ionization on these nonradiative pathways are difficult

(49) Kuharski, R. A.; Chandler, D.; Montgomery, J. A., Jr.; Rabii, F.; Singer, S. J. *J. Phys. Chem.* **1988**, *92*, 3261–3267.
(50) Callis, P. R., to be published.
(51) Hasha, D. L.; Eguchi, T.; Jonas, J. *J. Am. Chem. Soc.* **1982**, *104*, 2290–2296.
(52) Kirby, E. P.; Steiner, R. F. *J. Phys. Chem.* **1970**, *74*, 4480–4490.
(53) Bazin, M.; Patterson, L. K.; Santus, R. *J. Phys. Chem.* **1983**, *87*, 189–190.
(54) Cowgill, R. W. *Biochim. Biophys. Acta* **1963**, *75*, 272–273.
(55) Sisido, M.; Tanaka, R.; Inai, Y.; Imanishi, Y. *J. Am. Chem. Soc.* **1989**, *111*, 6790–6796.
(56) Boens, N.; Janssens, L. D.; De Schryver, F. C. *Biophys. Chem.* **1989**, *33*, 77–90.
(57) Shizuka, H.; Serizawa, M.; Kobayashi, H.; Kameta, K.; Sugiyama, H.; Matsuura, T.; Saito, I. *J. Am. Chem. Soc.* **1988**, *110*, 1726–1732.
(58) Vander Donckt, E. *Bull. Soc. Chim. Belg.* **1969**, *78*, 69–75.
(59) Barkley, M. D.; Tilstra, L.; McMahon, L. P.; Vela, M. A.; McLaughlin, M. L. *Proc. SPIE Int. Soc. Opt. Eng.* **1990**, *1204*, 124–125.
(60) Overlap integrals for donor–acceptor pairs: W(1)-glycine, 1.00×10^{-20} cm^6 mol^{-1}; W(1)E-glycine ethyl ester, 5.46×10^{-21} cm^6 mol^{-1}.

to ascertain. The decay-associated emission spectra of the two conformers are almost identical. Thus, we do not expect large differences in internal conversion and intersystem crossing rates between conformers. Furthermore, we can estimate the intersystem crossing rate k_{isc} from the temperature-independent rate k_o and the radiative rate k_r, where $k_o = k_r + k_{isc}$. Using data from Table VI [neglecting the nonlinear fit for τ_1 of W(1)E] and radiative rates calculated from quantum yields and mean lifetimes,[59] we obtain intersystem crossing rates of $\sim 5 \times 10^7$ s^{-1} for W(1) and W(1)E. Clearly, small changes in intersystem crossing rate would not account for the difference in lifetimes between conformers. Finally, the Arrhenius data argue that electron transfer is also occurring. The rate of transfer is expected to depend upon distance and perhaps also orientation of the carboxylate relative to the indole ring. It is satisfying that the shorter lifetime component can be associated with the conformer whose carboxylate is nearer the ring. Since the through-bond distance is the same in both conformers, the different lifetimes imply that the electron transfer is through-space. To better our understanding of quenching mechanisms in indole and tryptophan we are currently investigating solvent isotope effects in W(1) and related compounds.

Acknowledgment. We thank Dr. Marco A. Vela for chemical synthesis and HPLC and Dr. Mark L. McLaughlin for helpful discussion. This work was supported by NIH Grants GM35009 and GM42101.

Registry No. W(1), 42438-90-4; W(1)·H_2O, 129848-94-8; W(1)E, 129848-93-7.

Supplementary Material Available: Tables of (I) bond distances, (II) coordinates for hydrogen atoms, (III) bond distances involving hydrogen atoms, (IV) bond angles involving hydrogen, (V) torsion angles, (VI) anisotropic thermal parameters, (VIII) atomic point charges from 3-21G, (IX) defined force constants for atom types assigned in Figure S1, and (X) statistical comparison between geometric parameters of global minimum MM2 and X-ray structures of W(1) zwitterion (12 pages); listing of structure factor amplitudes (×10) (8 pages). Ordering information is given on any current masthead page.

Electron-Rich Iridium Complexes with Mixed-Donor Polydentate Ligands. Chemoselective Catalysts in Hydrogen-Transfer Reduction of α,β-Unsaturated Ketones

Claudio Bianchini,*,† Erica Farnetti,‡ Mauro Graziani,*,‡ Giorgio Nardin,‡ Alberto Vacca,† and Fabrizio Zanobini†

Contribution from the Dipartimento di Scienze Chimiche, Università di Trieste, Piazzale Europa 1, 34126 Trieste, Italy, and Istituto per lo Studio della Stereochimica ed Energetica dei Composti di Coordinazione del CNR, Via J. Nardi 39, 50132 Firenze, Italy.
Received April 30, 1990

Abstract: The mixed-donor polydentate ligands Pr^n-$N(CH_2CH_2PPh_2)_2$ (PNP) and $Et_2NCH_2CH_2N(CH_2CH_2PPh_2)_2$ (P_2N_2) react in THF with $[Ir(cod)(OMe)]_2$ (cod = cycloocta-1,5-diene) yielding the σ,η^2-cyclooctenyl complexes $[(PNP)Ir(\sigma,\eta^2\text{-}C_8H_{13})]$ (**1**) and $[(P_2N_2)Ir(\sigma,\eta^2\text{-}C_8H_{13})]$ (**2**). The crystal structure of **1** has been determined by X-ray methods. The iridium atom is coordinated to the phosphorus and nitrogen donors of PNP and to a cyclooctenyl group via σ and η bonding in a distorted trigonal-bipyramidal geometry. The same coordination geometry is assigned to the P_2N_2 derivative that exhibits a free diethylamino group. In solution, above ca. −30 °C, compounds **1** and **2** are in equilibrium with the hydride η^4-cod isomers $[(PNP)IrH(\eta^4\text{-cod})]$ (**3**) and $[(P_2N_2)IrH(\eta^4\text{-cod})]$ (**4**) via a β-H elimination/hydride migration pathway. The equilibrium constants for the **1** ⇄ **3** and **2** ⇄ **4** interconversions have been obtained at different temperatures by ^{31}P NMR integration in the range 298–348 K. The thermodynamic functions $\Delta H°$ and $\Delta S°$ for the **1** ⇄ **3** and **2** ⇄ **4** isomerization reactions have been calculated. They are rather similar with each other, but the enthalpy contribution appears slightly more favorable for the latter reaction, in nice accord with the higher concentration of the hydride species observed for the P_2N_2 system at comparable temperatures. Compounds **1** and **2** are good catalyst precursors for the chemoselective hydrogen-transfer reduction of α,β-unsaturated ketones such as benzylideneacetone to allylic alcohols. The catalytic activity of **1** and **2** has been compared and contrasted to that exhibited by the system "$[Ir(cod)(OMe)]_2$ + PNP or P_2N_2" prepared in situ as well as other related complexes like $[(PNP)Ir(\eta^4\text{-cod})]BPh_4$ (**5**), $[(P_2N_2)Ir(\eta^4\text{-cod})]BPh_4$ (**6**), $[(triphos)Ir(\sigma,\eta^2\text{-}C_8H_{13})]$ (**7**) and $[(triphos)Ir(\sigma,\eta^2\text{-}C_8H_{13})]BPh_4$ (**8**) [triphos = $MeC(CH_2PPh_2)_3$]. Through this comparison, valuable mechanistic information on the catalysis cycle has been obtained.

High electron density at the metal center seems to be an essential requisite for catalysts capable of selectively reducing α,β-unsaturated ketones to unsaturated alcohols via hydrogen transfer. In particular, the chemoselectivity has been related to the ability of electron-rich metal species to form M–H bonds exhibiting remarkable hydridic character.[1] As a matter of fact, it is not incidental that iridium and tertiary phosphines contribute the essential ingredients in several catalysis systems for such reactions.[2] A particular role appears to be played by bidentate, mixed N, P-donor ligands like Ph_2P-o-C_6H_4-NR_2, as they are known to form excellent iridium catalysts for the chemoselective reduction of α,β-unsaturated ketones.[3] The combination of soft and hard donor atoms, as it occurs in aminophosphine ligands, attracted our attention. In fact, one cannot exclude a priori that free coordination sites may be provided during the catalysis cycle

† ISSECC, CNR.
‡ University of Trieste.

(1) Nakano, T.; Umano, S.; Kino, Y.; Ishii, Y.; Ogano, M. *J. Org. Chem.* **1988**, *53*, 3752.
(2) Rauchfuss, T. B.; Roudhill, D. M. *J. Am. Chem. Soc.* **1974**, *96*, 3098.
(3) Farnetti, E.; Nardin, G.; Graziani, M. *J. Chem. Soc., Chem. Commun.* **1989**, 1264.

0002-7863/90/1512-9190$02.50/0